

## Recombinant Fibrinogen Vlissingen/Frankfurt IV

THE DELETION OF RESIDUES 319 AND 320 FROM THE  $\gamma$  CHAIN OF FIBRINOGEN ALTERS CALCIUM BINDING, FIBRIN POLYMERIZATION, CROSS-LINKING, AND PLATELET AGGREGATION\*

Received for publication, February 28, 2000, and in revised form, March 29, 2000  
Published, JBC Papers in Press, March 30, 2000, DOI 10.1047/jbc.M001618200

Kelly A. Hogan<sup>‡</sup>, Oleg V. Gorkun<sup>‡</sup>, Karim C. Lounes<sup>‡</sup>, Andrew I. Coates<sup>§</sup>, John W. Weisel<sup>¶</sup>,  
Roy R. Hantgan<sup>||</sup>, and Susan T. Lord<sup>‡§\*\*\*‡‡</sup>

From the <sup>‡</sup>Department of Pathology and Laboratory Medicine and the <sup>§</sup>Department of Chemistry and the  
<sup>\*\*</sup>Curriculum of Genetics and Molecular Biology, University of North Carolina, Chapel Hill, North Carolina 27599-7525,  
the <sup>¶</sup>Department of Cell and Developmental Biology, University of Pennsylvania, Philadelphia, Pennsylvania 19104,  
and <sup>||</sup>Wake Forest University School of Medicine, Winston-Salem, North Carolina 27157-1019

We synthesized a variant, recombinant fibrinogen modeled after the heterozygous dysfibrinogen Vlissingen/Frankfurt IV, a deletion of two residues,  $\gamma$ Asn-319 and  $\gamma$ Asp-320, located within the high affinity calcium-binding pocket. Turbidity studies showed no evidence of fibrin polymerization, although size exclusion chromatography, transmission electron microscopy, and dynamic light scattering studies showed small aggregates. These aggregates did not resemble normal protofibrils nor did they clot. Fibrinopeptide A release was normal, whereas fibrinopeptide B release was delayed approximately 3-fold. Plasmin cleavage of this fibrinogen was not changed by the presence of calcium or Gly-Pro-Arg-Pro, indicating that both the calcium-binding site and the “a” polymerization site were non-functional. We conclude that the loss of normal polymerization was due to the lack of “A-a” interactions. Moreover, functions associated with the C-terminal end of the  $\gamma$  chain, such as platelet aggregation and factor XIII cross-linking, were also disrupted, suggesting that this deletion of two residues affected the overall structure of the C-terminal domain of the  $\gamma$  chain.

Fibrinogen is a 340-kDa glycoprotein that consists of six polypeptide chains, ( $A\alpha$ ,  $B\beta$ , and  $\gamma$ )<sub>2</sub>. The molecule is symmetric, consisting of two globular D nodules connected to a central E nodule by a coiled-coil region (1). The D nodule consists of a portion of the coiled-coil region and the C termini of both the  $B\beta$  and  $\gamma$  chains, whereas the E nodule consists of the N termini of all six polypeptides. Thrombin cleaves the N termini of both the  $A\alpha$  and the  $B\beta$  chains, releasing fibrinopeptides A (FpA)<sup>1</sup> and B (FpB) and producing fibrin monomers that polymerize to form a fibrin clot. FpA is released first, exposing the polymerization site “A” that binds to the polymerization site “a” in the  $\gamma$  chain in the D domain of another molecule (2). This “A-a” interaction

allows molecules to align into double-stranded, half-staggered protofibrils (3, 4). It is unclear by what molecular mechanism FpB release affects polymerization, although a commonly accepted model proposes that FpB is released from growing protofibrils, enhancing the assembly of protofibrils into fibers (5–7). Release of FpB exposes the “B” polymerization site that binds to the “b” site (2), which may be located in the  $B\beta$  chain (8, 9) or the  $A\alpha$  chain (10). *In vivo*, the result of fibrin polymerization is an intricate fibrous network that, along with platelets, forms a hemostatic plug (11).

X-ray crystallography studies have defined several important residues of the C-terminal domain of the  $\gamma$  chain. When the peptide Gly-Pro-Arg-Pro (GPRP), which mimics the “A” site, was co-crystallized with either two covalently linked D nodules (12) or the  $\gamma$  C-terminal fragment of the D nodule (13), side chains from amino acids Gln-329, Asp-330, and Asp-364 were shown to interact with the peptide, forming the “a” site. Two of the three high affinity calcium-binding sites in fibrinogen (14, 15) are in the individual C termini of the  $\gamma$  chains. These  $\gamma$  chain calcium-binding sites lie adjacent to the polymerization pocket “a” (12, 13, 16). The specific residues that bind calcium are Asp-318, Asp-320, Phe-322, and Gly-324 (16). The structure of the last 14 residues of the C terminus of the  $\gamma$  chain ( $\gamma$ 398– $\gamma$ 411) has been difficult to resolve. Crystallography of a 30-kDa fragment of  $\gamma$  chain provided information through residue 401 (16); the last residue resolved in the structure of the 80-kDa fragment D was 398 (12). Nonetheless, biochemical studies have shown that the sites necessary for factor XIII (FXIII)  $\gamma$  chain cross-linking and platelet aggregation reside in these C-terminal residues. Specifically, FXIII forms a covalent bond between  $\gamma$ Gln-398 on one molecule and  $\gamma$ Lys-406 from another molecule (17). The last four residues,  $\gamma$ 408–411, are required for platelet aggregation (18).

We have synthesized the recombinant fibrinogen,  $\gamma\Delta$ 319,320, modeled after the heterozygous dysfibrinogen Vlissingen/Frankfurt IV (V/F IV), in which residues  $\gamma$ Asn-319 and  $\gamma$ Asp-320 are absent. We found that calcium binding, fibrin polymerization, and platelet aggregation were completely disrupted with the recombinant variant, in contrast to the plasma V/F IV fibrinogen, where functions were partially impaired (19). These results suggest that the overall structure of the  $\gamma$  C-terminal fragment has been altered.

### EXPERIMENTAL PROCEDURES

**Materials**—All chemicals were of reagent grade and, unless specified, were purchased from Sigma. Human  $\alpha$ -thrombin was purchased from Enzyme Research Laboratories, Inc. (South Bend, IN), and recombinant hirudin was purchased from Calbiochem-Novabiochem Corp. Factor XIII was a generous gift from Dr. Kevin Siebenlist (Sinai Samaritan

\* This work was supported by National Science Foundation Grant MCB 9728122 (to R. R. H.) and National Institutes of Health Grants HL 30954 (to J. W. W.), HL 31048, and HL 52706 (to S. T. L.). The costs of publication of this article were defrayed in part by the payment of page charges. This article must therefore be hereby marked “advertisement” in accordance with 18 U.S.C. Section 1734 solely to indicate this fact.

<sup>‡‡</sup> To whom the correspondence should be addressed: Dept. of Pathology and Laboratory Medicine, University of North Carolina, Rm. 603 Brinkhous-Bullitt Bldg., CB 7525, Chapel Hill, NC 27599-7525. Tel.: 919-966-2617; Fax: 919-966-6718; E-mail: stl@med.unc.edu.

<sup>1</sup> The abbreviations used are: FpA, fibrinopeptide A; FpB, fibrinopeptide B; GPRP, Gly-Pro-Arg-Pro; FXIII, factor XIII; PAGE, polyacrylamide gel electrophoresis.

Medical Center, Milwaukee, WI). Plasminogen was purified from human plasma by the method previously described (20) and stored at  $-20^{\circ}\text{C}$ . Streptokinase was purchased from American Diagnostica (Greenwich, CT).

**Construction of the Vector and Expression of the Protein**—The expression vector pMLP- $\gamma$  contains the entire  $\gamma$  chain cDNA and has been described (21). The 6 base pairs coding for Asn-319 and Asp-320 were deleted by oligo-directed mutagenesis using the Transformer TM site-directed mutagenesis kit from CLONTECH Laboratories (Palo Alto, CA) based on the procedure described by Deng *et al.* (22). The primers used to construct the mutation have been described (23). Chinese hamster ovary cells, which expressed the human  $\alpha$  and  $\beta$  fibrinogen chains, were co-transfected with the mutant  $\gamma$  chain expression vector and a plasmid containing the selection gene, pMSV *his* (see Ref. 21 for details). Individual clones, secreting high amounts of fibrinogen as determined by enzyme-linked immunosorbent assay, were grown in serum-free medium in roller bottles for large scale protein expression. The medium was harvested; phenylmethylsulfonyl fluoride was added, and the medium was stored at  $-20$  or  $-70^{\circ}\text{C}$ .

**Purification of Recombinant Fibrinogen**—Both  $\gamma\Delta 319,320$  and normal recombinant fibrinogen (24) were purified by ammonium sulfate precipitation and immunoaffinity chromatography using IF-1 monoclonal antibody (Iatron Corp., Tokyo, Japan) conjugated to Sepharose 4B (see Refs. 24 and 25 for details). Proteins were dialyzed against 20 mM HEPES, pH 7.4, 150 mM NaCl (HEPES buffer), aliquoted, and stored at  $-70^{\circ}\text{C}$ . To test the purity and assembly of the recombinant fibrinogen, proteins were analyzed by SDS-PAGE under reduced and non-reduced conditions by the method of Laemmli (26).

**Thrombin-catalyzed Fibrin Polymerization**—Polymerization was monitored at ambient temperature, and the change in turbidity at 350 nm using a Biospec 1601 spectrophotometer (Shimadzu Corp., Tokyo, Japan) was as described (24). Briefly, in a 100- $\mu\text{l}$  cuvette (Starna Cells, Inc., Alscadero, CA), 10  $\mu\text{l}$  of thrombin (0.5 units/ml) was added at zero time to 90  $\mu\text{l}$  of fibrinogen (0.11 mg/ml), in HEPES buffer containing 1 mM  $\text{CaCl}_2$ .

**Size Exclusion Chromatography**—Reactions were initiated by adding 10  $\mu\text{l}$  of thrombin (4 units/ml) to 90  $\mu\text{l}$  of fibrinogen (0.45 mg/ml). At specified time points, 1  $\mu\text{l}$  of hirudin (2,000 units/ml) was added to inhibit thrombin. Samples were immediately injected onto an Amersham Pharmacia Biotech HR 10/30 column packed with Superose 6 resin according to the manufacturer's instructions; this resin has a separation range from 5 to 5,000 kDa. The column was equilibrated with the reaction buffer (HEPES buffer containing 1 mM  $\text{CaCl}_2$ ). The products were eluted under constant flow at 1 ml/min and monitored at 280 nm. The void volume was determined with blue dextran 2,000 (Amersham Pharmacia Biotech).

**Plasmin Protection Assay and Western Blot**—Fibrinogen (0.1 mg/ml) was preincubated at ambient temperature for 15 min with EDTA (5 mM),  $\text{CaCl}_2$  (5 mM), or GPRP (2 mM). Meanwhile, 100  $\mu\text{l}$  of plasminogen (0.11 mg/ml) was activated with 10  $\mu\text{l}$  of streptokinase (10,000 units/ml) for 5 min, and 2  $\mu\text{l}$  was added to the fibrinogen samples (100  $\mu\text{l}$ ) and incubated overnight at  $37^{\circ}\text{C}$ . After incubation, the samples were run on a 7.5% SDS-PAGE gel, under non-reduced conditions, as described by Laemmli (26). The gel was electroblotted in 50 mM Tris, 380 mM glycine, 0.1% SDS, 20% methanol at 150 mA for 1.5 h to a nitrocellulose membrane (Micron Separations Inc, Westborough, MA). The membrane was blocked overnight at  $4^{\circ}\text{C}$  in TBS (20 mM Tris-HCl, pH 7.4, 150 mM NaCl) with 5% non-fat milk. Then it was incubated with a 1:10,000 dilution of rabbit polyclonal antiserum to fibrinogen (Dako, Carpinteria, CA) for 2 h in TBST (TBS with 0.05% Tween 20 (Aldrich)), containing 1% bovine serum albumin. The membrane was next washed three times with TBST and incubated with a 1:5000 dilution of goat anti-rabbit IgG conjugated to horseradish peroxidase (Calbiochem) for 1 h in TBST with 1% bovine serum albumin. The blot was washed three times and developed with ECL<sup>TM</sup> Western blotting Detection Reagent (Amersham Pharmacia Biotech).

**Thrombin-catalyzed Fibrinopeptide Release**—Reactions initiated by adding thrombin (either 0.01 or 0.005 units/ml) to fibrinogen (0.1 mg/ml) in HEPES buffer containing 1 mM  $\text{CaCl}_2$  were performed as described (27). Immediately after thrombin addition, the solutions were aliquoted, and at specified time points, the samples were boiled for 15 min to stop the reaction. The samples were centrifuged for 15 min at  $13,000 \times g$ , and the supernatants were stored at  $-70^{\circ}\text{C}$ . The amount of FpA and FpB in the supernatants was monitored by reverse phase high performance liquid chromatography. The FpA and FpB peak areas were calculated, and the data were fit to two successive first-order rate equations, and specificity constants,  $k_{\text{cat}}/K_m$ , were calculated as described (27). The means were compared by an unpaired *t* test using

Statview (Abacus Concepts, Berkeley, CA).

**Transmission Electron Microscopy**—Reactions were initiated by adding 3  $\mu\text{l}$  of thrombin (4 units/ml) to 27  $\mu\text{l}$  of fibrinogen (0.45 mg/ml, HEPES buffer containing 1 mM  $\text{CaCl}_2$ ). At specified time points, 5  $\mu\text{l}$  of the reaction was added to tubes containing 5  $\mu\text{l}$  of hirudin (4 units/ml). These samples were immediately diluted in 90  $\mu\text{l}$  of 50 mM ammonium formate, 70% glycerol, pH 7.4, and sprayed onto freshly cleaved mica. The samples were dried and rotary-shadowed with tungsten in a Denton Vacuum DV-502, as described previously (28–30). The shadowed protein films were picked up on 400 mesh copper grids and viewed on a LEO EM 910 transmission electron microscope.

**Isolation of Human Platelets and ADP-induced Aggregation**—The human platelets were isolated by the method previously described (18). Briefly, human blood was drawn into citrate, and the platelet-rich plasma was obtained by centrifugation at 800 rpm for 20 min. Prostaglandin E-1 (final concentration 20 nM) was added, and the sample was centrifuged again at 1800 rpm for 20 min. The pellet containing platelets was resuspended in Tyrode's buffer, pH 7.2 (10 mM HEPES, 135 mM NaCl, 2.7 mM KCl, 12 mM  $\text{NaHCO}_3$ , 5.5 mM glucose, 2% bovine serum albumin), and loaded onto a Sepharose CL-2B column. The platelets were eluted, and  $\text{CaCl}_2$  was added to 1 mM and  $\text{MgCl}_2$  added to 2 mM. For aggregation,  $2 \times 10^8$  platelets/ml were preincubated at  $37^{\circ}\text{C}$  with 250 nM fibrinogen, prior to activation with 10  $\mu\text{M}$  ADP. Aggregation of stirred solutions was monitored with a platelet aggregometer (Chrono-Log) as the increase in light transmission. Normal and  $\gamma\Delta 319,320$  fibrinogens were assayed three times with one platelet donor.

**FXIII Fibrin and Fibrinogen Cross-linking and Western Blot**—For fibrin cross-linking, each reaction contained 16  $\mu\text{l}$  of fibrinogen (0.375 mg/ml), 2  $\mu\text{l}$  of FXIII (0.04 mg/ml), and 2  $\mu\text{l}$  of thrombin (3 units/ml) in HEPES buffer containing 1 mM  $\text{CaCl}_2$ . After incubation at ambient temperature, the reaction was stopped with the addition of reducing buffer followed by boiling. For  $\gamma\Delta 319,320$  fibrinogen, an additional set of experiments was performed where 16  $\mu\text{l}$  of fibrinogen (0.375 mg/ml) was first incubated with 2  $\mu\text{l}$  of thrombin (3 units/ml) for 4 h. Next, 2  $\mu\text{l}$  of FXIII (40 units/ml) and 1  $\mu\text{l}$  of thrombin (3 units/ml) were added and incubated for the specified times. For fibrinogen cross-linking, 18  $\mu\text{l}$  of FXIII (0.67 mg/ml) and 18  $\mu\text{l}$  of thrombin (20 units/ml) were mixed in the presence of HEPES buffer containing 1 mM  $\text{CaCl}_2$  and incubated at  $37^{\circ}\text{C}$  for 35 min to activate the FXIII. Thrombin was inhibited by incubating with 12  $\mu\text{l}$  of hirudin (450 units/ml) at ambient temperature for 1 min. Four  $\mu\text{l}$  of the FXIIIa mix was added to 16  $\mu\text{l}$  fibrinogen (0.375 mg/ml) and incubated at ambient temperature for the specified times. All cross-linked products were analyzed on 7.5% reduced gels, electrophoresed, and blotted as described for the plasmin protection assay.

**Dynamic Light Scattering**—The variant  $\gamma\Delta 319,320$  fibrinogen was further purified by gel filtration chromatography with an Amersham Pharmacia Biotech 10/50 HR column packed with Superose 6B resin. The elution buffer was HEPES buffer, and the flow rate was 1 ml/min. Peak fractions were collected, concentrated using a Millipore Ultra-free<sup>®</sup> centrifugal filter device (Millipore Corp., Bedford, MA), and used for polymerization. All fibrinogen solutions were filtered using a 0.2- $\mu\text{m}$  Millipore filter before use to remove dust. Light-scattering intensity *versus* time measurements were performed using a 35-milliwatt He-Ne laser (model 120, Spectra Physics Inc., Mountain View, CA), a red-sensitive photomultiplier tube (R298P, Hamatsu, Middlesex, NJ), and a Brookhaven Instruments BI200 SM goniometer at a  $90^{\circ}$  angle (31, 32). For dynamic light scattering, a 72-channel digital correlator (BI-2030 AT, Brookhaven Instruments) was used with a "multiple sample times" option to divide each channel into four distinct real-time bases, allowing for an expanded decay time collection range. Data were acquired using the program BI-30ATN, and the resultant auto-correlation functions were analyzed employing cumulants analysis to obtain *z*-average translational diffusion coefficients (33–35) and the CONTIN algorithm to obtain size distributions (36). Polymerizations were performed at 0.2 mg/ml fibrinogen, 0.3 units/ml thrombin in HEPES buffer. Time-averaged intensities were taken incrementally for 4 h.

## RESULTS

### Characterization of the Purified $\gamma\Delta 319,320$ Fibrinogen

The recombinant fibrinogen  $\gamma\Delta 319,320$  was synthesized and purified as described under "Experimental Procedures." SDS-PAGE performed under non-reduced conditions demonstrated that the variant fibrinogen was pure and that it was assembled into the 340-kDa molecule (data not shown). A reduced gel showed that all three chains were produced and were intact (Fig. 1). As previously demonstrated with the plasma fibrino-

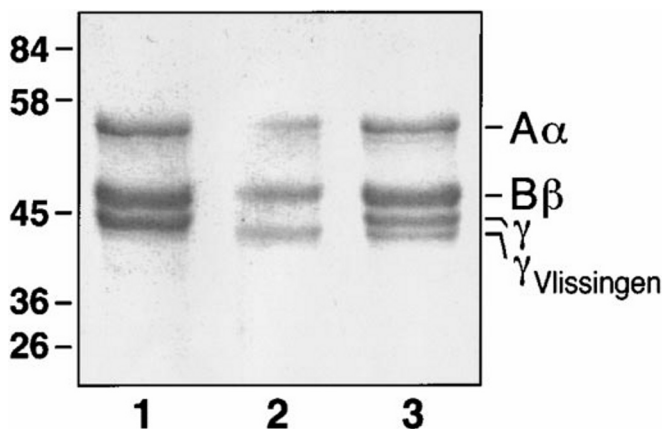


FIG. 1. **Characterization of  $\gamma\Delta 319,320$  fibrinogen.** SDS-PAGE gel (10%) was run under reduced conditions and stained with Coomassie Brilliant Blue (26). Lane 1, normal recombinant fibrinogen; lane 2,  $\gamma\Delta 319,320$  fibrinogen; lane 3, 1:1 mix of normal and  $\gamma\Delta 319,320$  fibrinogen.

gen V/F IV (19), the variant  $\gamma$  chain (lane 2) had a different mobility than the normal  $\gamma$  chain (lane 1). The difference in mobility was clearly seen in lane 3, with a 1:1 mix of normal and variant  $\gamma$  chain.

#### "A-a" Interactions Are Missing in $\gamma\Delta 319,320$ Fibrin

**Turbidity Studies**—Thrombin-catalyzed polymerization was monitored as turbidity at 350 nm. Under conditions where normal fibrinogen polymerized rapidly,  $\gamma\Delta 319,320$  fibrinogen did not show a rise in turbidity (Fig. 2). Additional experiments (data not shown) were performed under varied conditions that augment polymerization. Nevertheless, no turbidity change was detected with  $\gamma\Delta 319,320$  fibrinogen, even when the thrombin concentration was increased to 10 units/ml, the fibrinogen concentration was increased to 1.3 mg/ml, the temperature was lowered to 14 °C, the duration of the experiment was extended to 14 h, or the calcium concentration was raised to 10 mM.

**Fibrinopeptide Release**—To test whether the polymerization curves resulted from a blocked "A" site, we measured fibrinopeptide A and B release from normal and  $\gamma\Delta 319,320$  fibrinogen over a 2-h time course. The data were fit to two successive first-order rate equations under the assumption that FpA was released before FpB (37). Fig. 3 shows that indeed both FpA and FpB were released from  $\gamma\Delta 319,320$  fibrinogen, but the release of FpB was delayed relative to normal fibrinogen. The kinetic data presented in Table I show that FpA was released at a normal rate, whereas FpB was released at a rate about 3-fold slower than normal. The delayed release of FpB indicates that protofibril formation was impaired, as the release of FpB is reported to be accelerated by protofibril formation (5).

**GPRP Protection**—To determine whether the "a" site was functional in  $\gamma\Delta 319,320$  fibrinogen, we examined plasmin cleavage in the presence of GPRP, which mimics the "A" site (38). After incubating  $\gamma\Delta 319,320$  or normal fibrinogen with GPRP, we performed a plasmin digest as described under "Experimental Procedures." As shown in Fig. 4, normal fibrinogen was protected from plasmin cleavage by the presence of GPRP (lane 3), as the product labeled D1 remained. Normal fibrinogen was also protected from cleavage in the presence of 5 mM  $\text{CaCl}_2$  (lane 4), as described previously (39). In the absence of calcium or GPRP (lane 1), plasmin cleavage was demonstrated by the loss of the D1 product and the appearance of D2 and D3, as described previously (39, 40). We examined plasmin cleavage of  $\gamma\Delta 319,320$  fibrinogen under all three conditions and found no protection from plasmin cleavage as evidenced by the D2 and D3 products (lanes 6–8). Because the two-residue de-

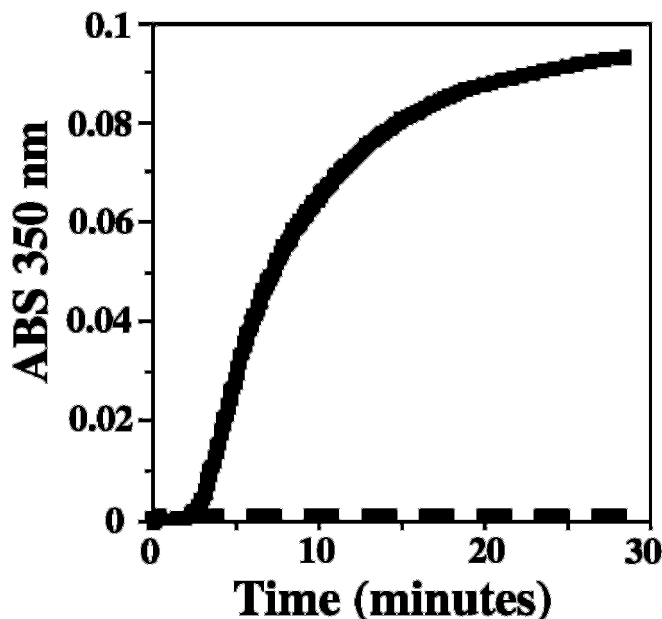


FIG. 2. **Polymerization of normal and  $\gamma\Delta 319,320$  fibrin.** Representative turbidity curves of 0.1 mg/ml fibrin (normal or  $\gamma\Delta 319,320$ ) polymerized by 0.05 units/ml thrombin in the presence of 1 mM  $\text{CaCl}_2$  are shown. Solid line, normal fibrin; dashed line,  $\gamma\Delta 319,320$  fibrin.

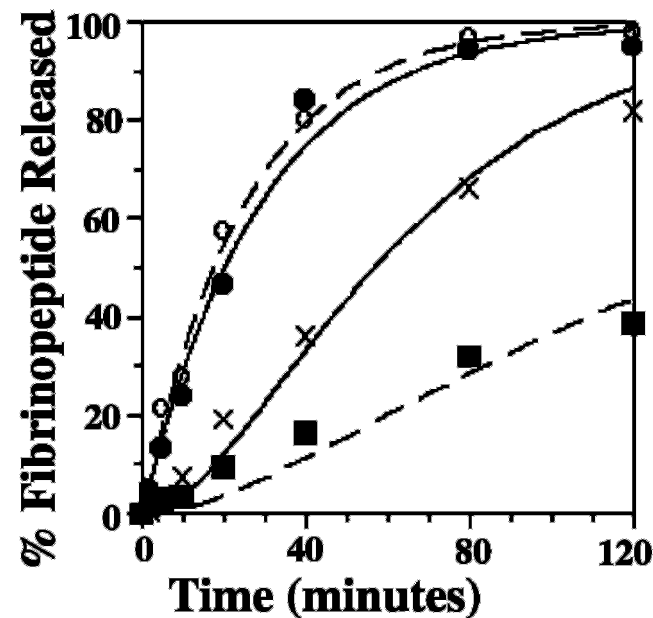


FIG. 3. **Fibrinopeptide release of normal and  $\gamma\Delta 319,320$  fibrinogen.** Representative data for the thrombin-initiated time course of fibrinopeptide A (● and ○) and fibrinopeptide B (× and ■) are shown. J, I, and solid line represent normal fibrinogen; E, B, and dashed line represent  $\gamma\Delta 319,320$  fibrinogen. Reactions were initiated by adding 0.005 units/ml thrombin to 0.1 mg/ml fibrinogen. The lines represent the best fit of the data into the equation as described (37).

letion removed part of the high affinity calcium-binding site (13, 16), it was not surprising that calcium provided no protection to  $\gamma\Delta 319,320$  fibrinogen (lane 8), similar to data obtained with plasma V/F IV (19). We conclude from the plasmin cleavage profile that GPRP did not bind to  $\gamma\Delta 319,320$  fibrinogen.

**$\gamma\Delta 319,320$  Fibrin Monomers Interact to Form Small Aggregates**—We further examined the polymerization of  $\gamma\Delta 319,320$  fibrin by size exclusion chromatography to determine whether products larger than fibrin monomers were formed (Fig. 5). At various time points, thrombin was inhibited, and the reaction products were immediately



TABLE I  
Specificity constants ( $K_{cat}/K_m$ ) for fibrinopeptide release

The units are  $10^{-6} \text{ M}^{-1} \text{ s}^{-1}$ . The average of three experiments is shown  $\pm$  the standard deviation.

Fibrinogen	Fibrinopeptide	$K_{cat}/K_m$	$p$ value
Normal	FpA	$12 \pm 6$	1.0
$\gamma\Delta 319, 320$	FpA	$12 \pm 4$	
Normal	FpB	$6.8 \pm 2.3$	0.03 <sup>a</sup>
$\gamma\Delta 319, 320$	FpB	$2.2 \pm 0.6$	

<sup>a</sup> Represents a significant  $p$  value.

run on a size exclusion column.

When thrombin was added to normal fibrinogen, polymerization was evident almost instantly. A peak at the void volume was seen as early as 28 s (data not shown), and a small monomer peak was still evident at 1 min (Fig. 5, *panel B*). After 3 min, a monomer peak was not detected (*panel C*), and only a small peak at the void volume was seen. With  $\gamma\Delta 319,320$  fibrinogen, the result was quite different. At 3 min (*panel E*), most of the protein was still in the monomer peak. A peak at the void volume was not seen until 30 min (data not shown), and after 240 min (*panel F*), the monomer peak was still evident. The void volume peak was not present when  $\gamma\Delta 319,320$  fibrinogen was incubated with inhibited thrombin for 240 min (data not shown), ensuring that the formation of high molecular components was thrombin-dependent.

Finally, we observed that the size distribution of larger species was different between the normal and  $\gamma\Delta 319,320$  fibrin. For example, at 1 min, normal fibrinogen had two distinctive fractions represented by two peaks with little material between the two peaks. In contrast, at 240 min,  $\gamma\Delta 319,320$  fibrin had two major peaks, but there was also evidence of a broad spectrum of material between these two peaks. We concluded that  $\gamma\Delta 319,320$  fibrin is capable of forming higher molecular weight species, although the nature of this material could not be determined by size exclusion chromatography.

**Transmission Electron Microscopy**—To characterize this high molecular weight material, we used transmission electron microscopy. We performed reactions as for size exclusion chromatography, inhibited thrombin at specific times, and immediately diluted and sprayed the solutions onto mica. The samples were visualized by rotary shadowing with tungsten (Fig. 6). Under these conditions, normal fibrin became a gel within 1 min, such that at 1 min and thereafter only the unclottable/soluble fraction of normal fibrin was visible by transmission electron microscopy, and the microscopic fields were sparsely populated with molecules (Fig. 6, *panel C*). We limited our analysis of normal fibrin to time points  $\leq 1$  min, and we assumed that the discernible fibrin monomers and aggregates were those that did not incorporate into the clot. In contrast, under these conditions  $\gamma\Delta 319,320$  fibrin did not form a gel, and over the 4-h incubation, microscopic fields remained densely populated with molecules (Fig. 6, *panel D*).

As can be seen in Fig. 6, the  $\gamma\Delta 319,320$  fibrinogen molecules (*panel B*) appeared the same as normal fibrinogen molecules (*panel A*); most  $\gamma\Delta 319,320$  fibrinogen molecules appeared trinodular, and the majority of molecules were monomeric, and there were no obvious abnormal structures. Following incubation with thrombin, both normal and  $\gamma\Delta 319,320$  fibrin demonstrated a shift in the population of molecules seen. We analyzed many fields, counted the number of molecules, and scored these as monomers, pairs, or aggregates (Table II). Paired molecules were defined as two molecules touching each other in any orientation, whereas aggregates were defined as a group of three molecules or more. The data were expressed as a percentage of molecules (of total counted) in monomers, pairs, or aggregates, where, for example, the number of molecules counted

as pairs was twice the number of pairs. Aggregates from both normal and  $\gamma\Delta 319,320$  fibrin were scored as being either elongated, indicated by an *arrowhead*, or irregular-shaped, indicated by an *asterisk*, in Fig. 6, *panels E* and *F*. Often, it was difficult to discern if a nodule belonged to one molecule or another, so the number of monomers per aggregate was based on an estimate of the total number of nodules seen (one molecule is tri-nodular). Consistent with the chromatography data, after a 4-h incubation, the fraction of  $\gamma\Delta 319,320$  fibrin monomers decreased and the fraction of oligomers increased. Although there were no striking differences between normal and  $\gamma\Delta 319,320$  aggregates, analysis of the electron microscopy data showed that more elongated aggregates were seen with  $\gamma\Delta 319,320$  fibrin than in normal fibrin (Table II). From the microscopy data, we conclude that after prolonged incubation  $\gamma\Delta 319,320$  fibrin formed aggregates, that these aggregates were small (on average, four or fewer monomers), and that a significant fraction of aggregates (about 40% at 4 h) were elongated as might be expected for early polymerization.

**Dynamic Light Scattering**—Because both size exclusion chromatography and transmission electron microscopy only examined the molecules/aggregates that remained soluble, we also examined polymerization by dynamic light scattering which analyzed all products in a closed system. This method provided time-correlated molecular mass and diffusion coefficient data, which we compared with corresponding data for normal fibrinogen (41). Under the conditions of our assay, within 20 s, analysis of the data with normal fibrin would show a 6–10-fold increase in molecular mass and a 10-fold drop in the diffusion coefficient, consistent with formation of elongated, rod-shaped structures, that is, protofibrils (41). When we examined  $\gamma\Delta 319,320$  fibrin by dynamic light scattering (Fig. 7), the results were significantly different from normal. The molecular mass increased only 2-fold, on average, and the diffusion coefficient dropped about 1.5-fold after 4 h. These data were consistent with the formation of small aggregates, consisting on average of  $3.9 \pm 2.5$  fibrin monomers per aggregate. We conclude that the light scattering data and the results seen by electron microscopy demonstrated that only small aggregates of fibrin were formed.

#### Distant Functional Sites in Fibrinogen Are Affected by the $\gamma\Delta 319,320$ Deletion

**Fibrin Cross-linking**—We also investigated other  $\gamma$  chain coagulation functions, including fibrin cross-linking by the transglutaminase, FXIII. During polymerization, factor XIII is activated by thrombin to FXIIIa, which catalyzes the formation of a covalent bond between Gln and Lys of two  $\gamma$  chains (17) or two or more  $\alpha$  chains (42). We examined cross-link formation by incubating fibrinogen, thrombin, and FXIII, and analyzing the products on immunoblots from SDS gels run under reducing conditions. As shown in Fig. 8, with normal fibrinogen, the formation of  $\gamma$ - $\gamma$  dimers was essentially complete after a 5-min incubation (*lane 2*). With longer incubation, the  $\gamma$  chain completely disappeared as  $\gamma$ - $\gamma$  dimers formed, and the  $\alpha$  chain disappeared, indicating the formation of  $\alpha$ -polymers. With  $\gamma\Delta 319,320$  fibrinogen, cross-linking was clearly impaired. After a 4-h incubation, a faint  $\gamma$ - $\gamma$  dimer band was obvious as was a decrease in both the  $\alpha$  and  $\gamma$  chains (*lane 10*). After 24 h (*lane 16*), the  $\gamma$ - $\gamma$  dimer band was still faint, and the  $\gamma$  chain band had faded, but the  $\alpha$  chain had completely disappeared. Because we might expect fibrin cross-linking to be impaired with monomers that did not polymerize, we also examined cross-linking after  $\gamma\Delta 319,320$  fibrinogen was incubated first with thrombin for 4 h, followed by addition of FXIII (*lanes 11–15*). The immunoblot demonstrated that cross-linking of  $\gamma\Delta 319,320$

FIG. 4. **Plasmin protection assay.** A non-reduced 7.5% SDS-PAGE gel (26) was immunoblotted with a polyclonal anti-fibrinogen antibody. Normal (lanes 1–4) or  $\gamma\Delta 319,320$  (lanes 5–8) fibrinogen was incubated with plasmin overnight in the presence of 5 mM EDTA, 5 mM  $\text{CaCl}_2$ , or 2 mM GPRP. Lanes 1 and 5, undigested fibrinogen; lanes 2 and 6, EDTA; lanes 3 and 7, GPRP; lanes 4 and 8,  $\text{CaCl}_2$ .

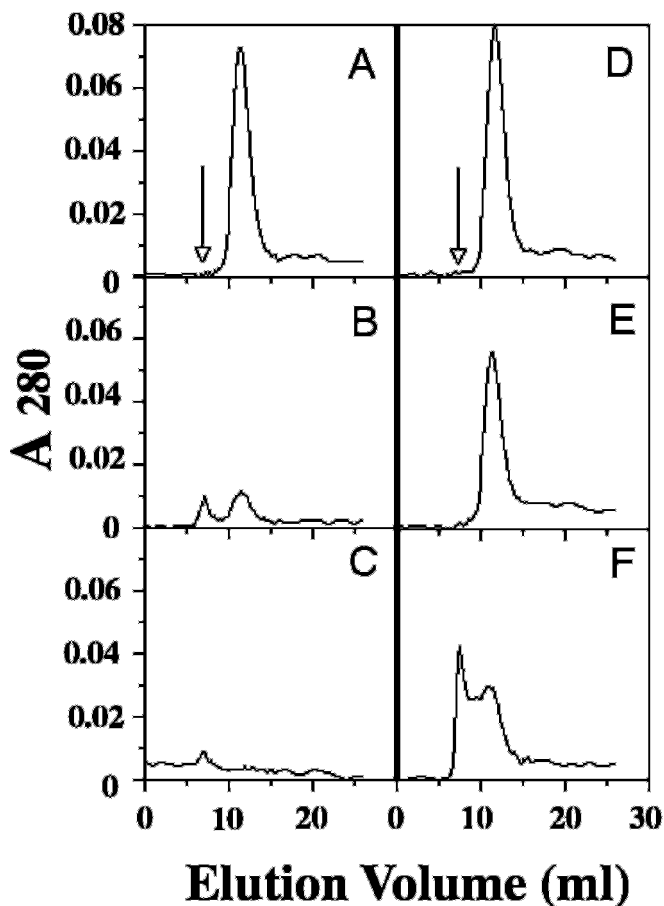
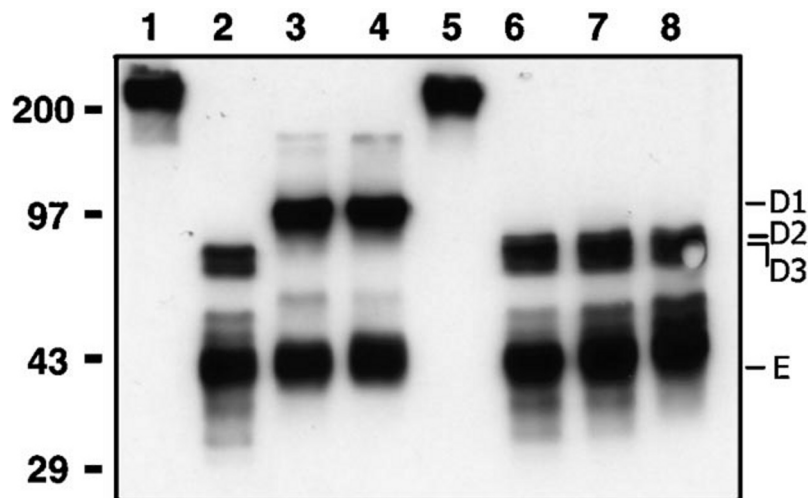


FIG. 5. **Size exclusion chromatography.** Thrombin was mixed with fibrinogen and incubated. After the addition of hirudin to inhibit thrombin, the sample was immediately run over an Amersham Pharmacia Biotech HR 10/30 column packed with Superose 6B. Panels A–C, normal fibrinogen after incubation for 0, 1, and 3 min, respectively. Panels D–F,  $\gamma\Delta 319,320$  fibrinogen after incubation for 0 and 3 min and 4 h, respectively. The arrows delineate the void volume.

fibrin was somewhat enhanced by prior incubation with thrombin, but the rate and extent of cross-link formation was still markedly impaired.

**Fibrinogen Cross-linking**—Although polymerizing fibrin is a better substrate, FXIIIa will also cross-link fibrinogen. In these experiments, we first activated FXIII and initiated the reaction by adding FXIIIa to fibrinogen, as described under “Experimental Procedures,” and analyzed the products by Western blot

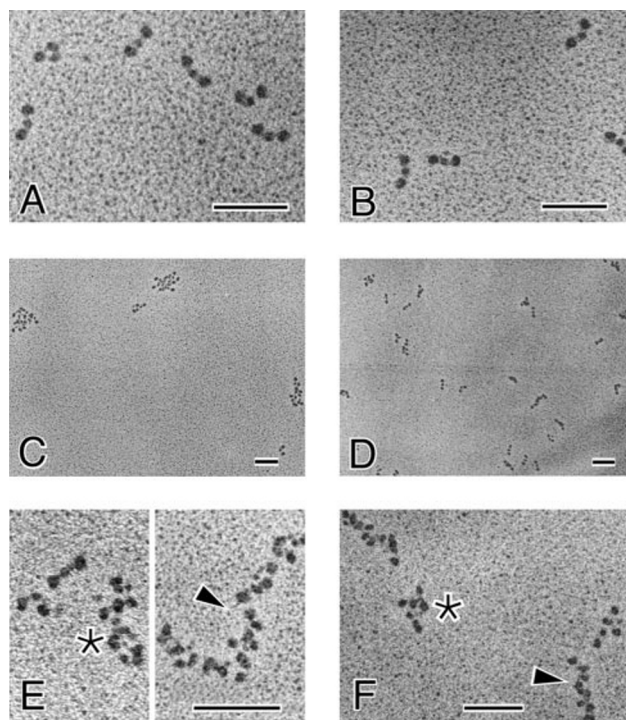


FIG. 6. **Transmission electron microscopy.** Thrombin was mixed with fibrinogen and incubated. After the addition of hirudin used to inhibit thrombin, the sample was immediately diluted and sprayed on mica. The mica samples were rotary shadowed with tungsten and viewed by transmission electron microscopy. Scale bars in all panels represent 95 nm. Panel A, normal fibrinogen; panel B,  $\gamma\Delta 319,320$  fibrinogen; panel C, representative field of normal fibrin 1 min after thrombin addition; panel D, representative field of  $\gamma\Delta 319,320$  fibrin 4 h post-thrombin addition; panel E, elongated (arrowhead) and irregular-shaped aggregates (asterisk) in normal fibrin, 1 min post-thrombin addition; panel F, elongated (arrowhead) and irregular-shaped aggregates (asterisk) in  $\gamma\Delta 319,320$  fibrin, 4 h post-thrombin addition.

(Fig. 9). After 1 h, with normal fibrinogen, the blot demonstrated complete loss of the  $\alpha$  chain, indicative of  $\alpha$ -polymer formation, and a strong  $\gamma$ - $\gamma$  dimer band. After 1 h, with  $\gamma\Delta 319,320$  fibrinogen, there was also complete loss of the  $\alpha$  chain, yet the  $\gamma$  chain band remained essentially unchanged, and no band representing  $\gamma$ - $\gamma$  dimers was seen. Even after 24 h, there was no evidence for  $\gamma$ - $\gamma$  dimer formation with  $\gamma\Delta 319,320$  fibrinogen (data not shown). We conclude that, specifically, the  $\gamma$  chain of  $\gamma\Delta 319,320$  fibrinogen was a very poor substrate for FXIIIa.

**Platelet Aggregation**—We also examined fibrinogen-mediated

TABLE II  
Population of molecules viewed by transmission electron microscopy

The total number of monomers was counted at each time point based on many views. The number of monomers in monomeric, paired, or aggregated form was expressed as a percentage.

Fibrin(ogen) time point	Total molecules counted	Monomers	Paired molecules <sup>a</sup>	Molecules in aggregates <sup>b</sup>	Percent of aggregates, elongated
Normal, 0 min	524	361 (69%)	104 (20%)	59 (11%)	20
Normal, 28 s	354	142 (40%)	90 (25%)	122 (34%)	9
$\gamma\Delta 319, 320, 0$ min	535	353 (66%)	144 (27%)	38 (7%)	12
$\gamma\Delta 319, 320, 3$ min	485	240 (49%)	162 (33%)	83 (17%)	29
$\gamma\Delta 319, 320, 2$ h	522	200 (38%)	134 (26%)	188 (36%)	47
$\gamma\Delta 319, 320, 4$ h	287	72 (25%)	90 (31%)	125 (43%)	39

<sup>a</sup> Represents molecules that were touching, in any orientation.

<sup>b</sup> Represents any group of three molecules or more.

FIG. 7. **Dynamic light scattering.** Fractional change in translational diffusion coefficient over time. Thrombin (0.3 units/ml) was added to purified  $\gamma\Delta 319,320$  fibrinogen (0.2 mg/ml) and monitored for 4 h.  $D/D_0$ , the normalized diffusion coefficient, is shown on one y axis, and size distributions (units are monomers of fibrin) are shown on the opposite y axis. Three reactions are shown.

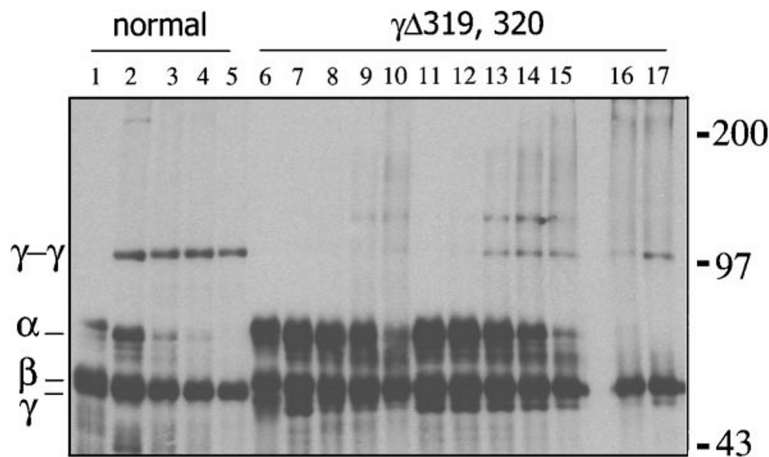
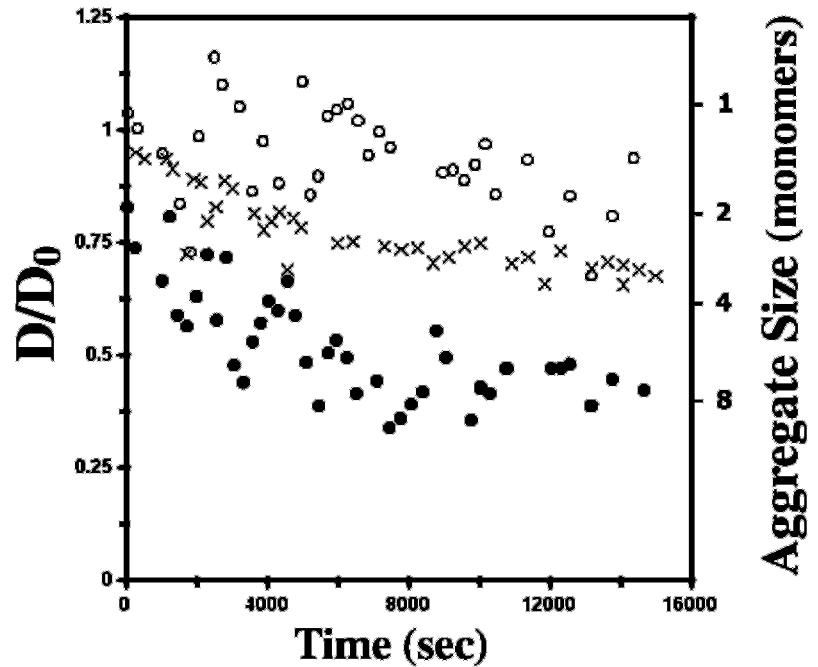


FIG. 8. **Fibrin cross-linking with FXIII.** Fibrinogen, thrombin, and factor XIII were mixed and incubated for 0, 5, or 20 min or 1 or 4 h. Lanes 1–5, normal fibrinogen; lanes 6–10,  $\gamma\Delta 319,320$  fibrin. Lanes 11–15 demonstrate a reaction in which only  $\gamma\Delta 319,320$  fibrinogen and thrombin were mixed and incubated for 4 h prior to the addition of factor XIII and incubation for 0, 5, or 20 min or 1 or 4 h. Lanes 16 and 17, 24-h time points for  $\gamma\Delta 319,320$  fibrin without and with prior thrombin incubation, respectively. A reduced 7.5% SDS-PAGE gel (26) was immunoblotted with a polyclonal anti-fibrinogen antibody. The blot was slightly overexposed to enhance the  $\gamma$ - $\gamma$  band signal.

ated platelet aggregation, the hemostatic function that requires the last four residues ( $\gamma 408$ –411) of the  $\gamma$  chain (18). We monitored ADP-induced platelet aggregation as a change in light transmission, as described under “Experimental Proce-

dures,” and the results are shown in Fig. 10. After ADP addition (indicated by arrows), we saw in both samples the expected decrease in light transmission that reflects the platelet shape change indicative of platelet activation. In the presence of



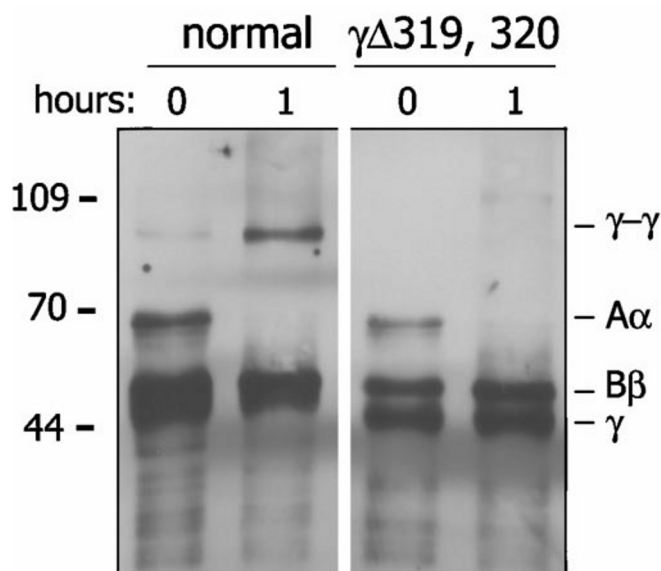


FIG. 9. Fibrinogen cross-linking in the absence of thrombin with activated FXIII. Normal or  $\gamma\Delta 319,320$  fibrinogen was incubated with pre-activated FXIII and the reaction was stopped after 1 h. A reduced 7.5% SDS-PAGE gel (26) was immunoblotted with a polyclonal anti-fibrinogen antibody. The blot was slightly overexposed to enhance the  $\gamma$ - $\gamma$  band signal.

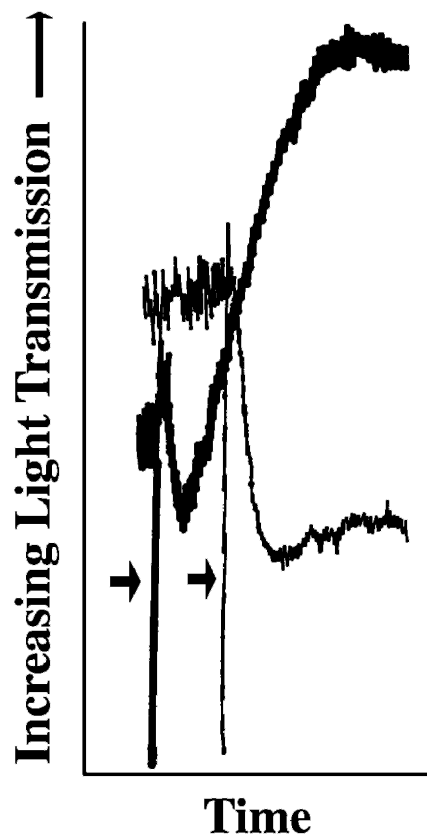


FIG. 10. ADP-induced platelet aggregation.  $2 \times 10^8$  platelets/ml were preincubated at 37 °C with 250 nM fibrinogen, prior to activation with 10  $\mu$ M ADP (indicated by arrows). Aggregation of stirred solutions was monitored as an increase in light transmission. Thick line, normal fibrinogen; thin line,  $\gamma\Delta 319,320$  fibrinogen.

normal fibrinogen, subsequent light transmission increased rapidly as the platelets aggregated and the solution became more transparent. In contrast, in the presence of  $\gamma\Delta 319,320$  fibrinogen, light transmission did not change after the initial

decrease. We conclude that  $\gamma\Delta 319,320$  fibrinogen did not support normal platelet aggregation.

#### DISCUSSION

We have synthesized the recombinant  $\gamma\Delta 319,320$  fibrinogen, modeled from the dysfibrinogen V/F IV, which was shown to be defective in calcium binding, fibrin polymerization, and platelet aggregation (19, 43). As with many dysfibrinogens expressed in heterozygous patients, however, the consequence of the mutation cannot be fully appreciated in the presence of normal molecules. Therefore, we synthesized the variant recombinant fibrinogen to study the effect of this two-residue deletion in the absence of normal molecules.

The data presented here suggest that the deletion of residues 319 and 320 affected the structural integrity of the C-terminal domain of the  $\gamma$  chain. Based on the crystallography data, it was reasonable that a deletion in the calcium binding pocket would have profound effects on the adjacent polymerization site, "a" (12, 13, 16). However, it was unexpected that functions associated with distant residues were also affected. The FXIIIa-catalyzed formation of  $\gamma$ - $\gamma$  dimers was severely impaired, with either  $\gamma\Delta 319,320$  fibrinogen or fibrin. Because  $\gamma$ - $\gamma$  dimers were not seen with fibrinogen, we concluded that the loss of function was inherent in the  $\gamma$  chain structure *per se* and not simply associated with the impaired polymerization of fibrin. In addition, ADP-induced, fibrinogen-mediated platelet aggregation was nonexistent. Previous studies suggest that the  $\gamma$  chain residues needed to support FXIIIa-catalyzed cross-linking and platelet aggregation are independent from the rest of the molecule (44–46). For example, a glutathione *S*-transferase chimeric protein containing residues  $\gamma 398$ –411 was able to bind to GPIIb/IIIa, the platelet receptor that mediates fibrinogen-dependent aggregation (46). This chimeric protein was also a substrate for FXIIIa, forming cross-linked dimers. The crystal structure of this chimeric protein suggested that this 14-residue segment of the  $\gamma$  chain has a flexible, "Z-shaped" structure, and when this structure was superimposed onto that from cross-linked fragment D, the residues involved in both platelet aggregation and FXIII cross-linking were available on the surface of the domain (46). We conclude, therefore, that in  $\gamma\Delta 319,320$  fibrinogen, these residues are either inaccessible or in an altered configuration. Perhaps these residues are buried in the  $\gamma\Delta 319,320$  fibrinogen molecule. Irrespective of the exact nature of the change, the data support the conclusion that the deletion of residues 319 and 320 altered the structure of these distant residues. We interpret these data as indicating that the overall structure of the C-terminal domain of the  $\gamma$  chain has been altered as a result of the two-residue deletion.

The experiments with  $\gamma\Delta 319,320$  demonstrated the value of studies on dysfibrinogens in a homogenous form. Polymerization of plasma fibrinogen V/F IV, purified from a heterozygous individual, was shown to be impaired (19), yet clotting of recombinant  $\gamma\Delta 319,320$  fibrinogen was undetectable. Importantly, we have identified a variant fibrinogen in which normal polymerization does not occur. Previous to these studies, every variant fibrinogen, whether recombinant or from plasma, has shown at least minimal polymerization by turbidity studies. Even fibrin with a substitution at a key residue in "a,"  $\gamma$ D364H, demonstrated a rise in turbidity by 60 min with 0.45 mg/ml fibrinogen and 0.5 units/ml thrombin (25). We saw no increase in turbidity under these same conditions.

The results from the size exclusion chromatography, electron microscopy, and light scattering support the conclusion that the very first step in polymerization was lost, and normal protofibrils were not formed. The elongated aggregates apparent with  $\gamma\Delta 319,320$  fibrin could be either short protofibrils that cannot laterally aggregate or aggregates that are coincident

tally elongated in shape, similar to protofibrils. We favor the latter based on their appearance in comparison to previously published transmission electron microscopy data of normal protofibrils (47, 48). Because aggregate formation was thrombin-dependent, interactions that are thrombin-dependent yet weaker than "A-a" may have a role. One potential interaction would follow the release of FpB, exposing the "B" site that can interact with the "b" site. Based on the structure of fragment D (12), we would expect "B-b" interactions to form unusual polymers, such as the oligomers seen in  $\gamma\Delta 319,320$  fibrin. Previous biochemical studies indicate that an interaction between "A" and "b" might lead to abnormal polymer forms (49), although crystallography studies did not detect any "A" binding to "b" (8). Another thrombin-dependent interaction may occur through the  $\alpha C$  domains, which contact each other and the central E nodule in fibrinogen (30, 50). In fibrin, the  $\alpha C$  domains separate from the center of the molecule (30), possibly uncovering new sites for intermolecular interactions. In transmission electron microscopy studies, Veklich *et al.* (30) identified fibrin aggregates that interact via their  $\alpha C$  domains. Similar aggregates were seen on occasion with  $\gamma\Delta 319,320$  fibrin (data not shown), so such interactions may support this abnormal polymer. Regardless of whether "B-b" or "A-b" or  $\alpha C$ - $\alpha C$  interactions mediate the formation of  $\gamma\Delta 319,320$  fibrin aggregates, the results provide evidence that without a functional "a", protofibrils, and consequently a fibrin clot, cannot form.

Our polymerization results also support one proposed model for the structure of  $\beta$ -fibrin, the product of cleavage by a protease that releases predominantly FpB. This fibrin polymer only forms at 14 °C (51), but it is normal in that there are normal protofibrils, fibers, and clots (6, 52). It has been proposed that  $\beta$ -fibrin is mediated through "B-a" interactions (8). As no turbidity changes were detected when  $\gamma\Delta 319,320$  fibrinogen was mixed with thrombin at 14 °C (data not shown), our data are consistent with this model of  $\beta$ -fibrin that requires a functional "a" site.

In summary, we have synthesized a recombinant fibrinogen modeled after the dysfibrinogen V/F IV, a deletion of residues  $\gamma 319$  and  $\gamma 320$ . The loss or impairment of several coagulation functions associated with the  $\gamma$  chain suggests that a significant change in structure has occurred in the molecule. Nonetheless, the deletion had no apparent effect on assembly or secretion, and transmission electron microscopy showed that the overall tri-nodular structure of the molecule was normal. Thus, we hypothesize that the deletion has induced a significant structural change only within the C-terminal domain of the  $\gamma$  chain.

**Acknowledgments**—We thank Li Fang Ping and Kasim McLain for their help in protein expression and purification; Mike Rooney for help with platelet purification and platelet aggregation; and Chandrasekaran Nagaswami for technical assistance with transmission electron microscopy preparation.

#### REFERENCES

- Brown, J. H., Volkman, N., Jun, G., Henschen-Edman, A. H., and Cohen, C. (2000) *Proc. Natl. Acad. Sci. U. S. A.* **97**, 85–90
- Budzynski, A. Z., and Olexa, S. A. (1980) *Proc. Natl. Acad. Sci. U. S. A.* **77**, 1374–1378
- Hantgan, R. R., and Hermans, J. (1979) *J. Biol. Chem.* **254**, 11272–11281
- Ferry, J. D. (1952) *Proc. Natl. Acad. Sci. U. S. A.* **38**, 566–569
- Blombäck, B., Hessel, B., Hogg, D., and Therkildsen, L. (1978) *Nature* **275**, 501–505
- Weisel, J. W. (1986) *Biophys. J.* **50**, 1079–1093
- Weisel, J. W., Veklich, Y. I., and Gorkun, O. V. (1993) *J. Mol. Biol.* **232**, 285–297
- Everse, S. J., Spraggon, G., Veerapandian, L., and Doolittle, R. F. (1999) *Biochemistry* **38**, 2941–2946
- Medved, L. V., Litvinovich, S. V., Ugarova, T. P., Lukinova, N. I., Kalikhevich, V. N., and Ardemasova, Z. A. (1993) *FEBS Lett.* **320**, 239–242
- Hasegawa, N., and Sasaki, S. (1990) *Thromb. Res.* **57**, 183–195
- Blombäck, B. (1996) *Thromb. Res.* **83**, 1–75
- Spraggon, G., Everse, S. J., and Doolittle, R. F. (1997) *Nature* **389**, 455–462
- Pratt, K. P., Coté, H. C. F., Chung, D. W., Stenkamp, R. E., and Davie, E. W. (1997) *Proc. Natl. Acad. Sci. U. S. A.* **94**, 7176–7181
- Marguerie, G., Chagniel, G., and Suscillon, M. (1977) *Biochim. Biophys. Acta* **490**, 94–103
- Nieuwenhuizen, W., and Haverkate, F. (1983) *Ann. N. Y. Acad. Sci.* **408**, 92–96
- Yee, V. C., Pratt, K. P., Coté, H. C. F., Le Trong, I., Chung, D. W., Davie, E. W., Stenkamp, R. E., and Teller, D. C. (1997) *Structure* **5**, 125–138
- Chen, R., and Doolittle, R. F. (1971) *Biochemistry* **10**, 4486–4491
- Rooney, M. M., Parise, L. V., and Lord, S. T. (1996) *J. Biol. Chem.* **271**, 8553–8555
- Koopman, J., Haverkate, F., Briet, E., and Lord, S. T. (1991) *J. Biol. Chem.* **266**, 13456–13461
- Deutsch, D. G., and Mertz, E. T. (1970) *Science* **170**, 1095–1096
- Binnie, C. G., Hettasch, J. M., Strickland, E., and Lord, S. T. (1993) *Biochemistry* **32**, 107–113
- Deng, W. P., and Nickloff, J. A. (1992) *Anal. Biochem.* **200**, 81–88
- Hogan, K. A., Lord, S. T., Okumura, N., Terasawa, F., Galanakis, D. K., Scharrer, I., and Gorkun, O. V. (2000) *Thromb. Haemostasis* **83**, 592–597
- Gorkun, O. V., Veklich, Y. I., Weisel, J. W., and Lord, S. T. (1997) *Blood* **89**, 4407–4414
- Okumura, N., Gorkun, O. V., and Lord, S. T. (1997) *J. Biol. Chem.* **272**, 29596–29601
- Laemmli, U. K. (1970) *Nature* **227**, 680–685
- Lord, S. T., Strickland, E., and Jayjock, E. (1996) *Biochemistry* **35**, 2342–2346
- Fowler, W. E., and Erickson, H. P. (1979) *J. Mol. Biol.* **134**, 241–249
- Weisel, J. W., Stauffacher, C. V., Bullitt, E., and Cohen, C. (1985) *Science* **230**, 1388–1391
- Veklich, Y. I., Gorkun, O. V., Medved, L. V., Nieuwenhuizen, W., and Weisel, J. W. (1993) *J. Biol. Chem.* **268**, 13577–13585
- Hantgan, R. R., Paumi, R., Rocco, M., and Weisel, J. W. (1999) *Biochemistry* **38**, 14461–14474
- Hantgan, R. R., Braaten, J. V., and Rocco, M. (1993) *Biochemistry* **32**, 3935–3941
- Koppel, D. E. (1972) *J. Chem. Phys.* **57**, 4814–4820
- Johnson, C. S., and Gabriel, D. A. (1981) in *Spectroscopy in Biochemistry* (Bell, J. E., ed) Vol. 2, pp. 177–272, CRC Press Inc., Boca Raton, FL
- Berne, B. J., and Pecora, R. (1990) *Dynamic Light Scattering: With Applications to Chemistry, Biology, and Physics*, R. E. Krieger, Malabar, FL
- Provencher, S. W. (1982) *Comput. Phys. Commun.* **27**, 213–227
- Ng, A. S., Lewis, S. D., and Shafer, J. A. (1993) *Methods Enzymol.* **222**, 341–358
- Laudano, A. P., and Doolittle, R. F. (1978) *Proc. Natl. Acad. Sci. U. S. A.* **75**, 3085–3089
- Haverkate, F., and Timan, G. (1977) *Thromb. Res.* **10**, 803–812
- Yamazumi, K., and Doolittle, R. F. (1992) *Protein Sci.* **1**, 1719–1720
- Knoll, D. A. (1983) *Applications of Light Scattering to the Study of Interactions of Biological Macromolecules*, Doctoral dissertation, University of North Carolina
- Mckee, P. A., Mattock, P., and Hill, R. L. (1970) *Proc. Natl. Acad. Sci. U. S. A.* **66**, 738–744
- Galanakis, D. K., Spitzer, S. G., Scharrer, I., and Peerschke, E. I. (1993) *Thromb. Haemostasis* **69**, 1261
- Kloczewiak, M., Timmons, S., Lukas, T. J., and Hawiger, J. (1984) *Biochemistry* **23**, 1767–1774
- Kloczewiak, M., Timmons, S., Bednarek, M. A., Sakon, M., and Hawiger, J. (1989) *Biochemistry* **28**, 2915–2919
- Ware, S., Donahue, J. P., Hawiger, J., and Anderson, W. F. (1999) *Protein Sci.* **8**, 2663–2671
- Fowler, W. E., Hantgan, R. R., Hermans, J., and Erickson, H. P. (1981) *Proc. Natl. Acad. Sci. U. S. A.* **78**, 4872–4876
- Medved, L., Ugarova, T., Veklich, Y., Lukinova, N., and Weisel, J. W. (1990) *J. Mol. Biol.* **216**, 503–509
- Laudano, A. P., and Doolittle, R. F. (1980) *Biochemistry* **19**, 1013–1019
- Gorkun, O. V., Veklich, Y. I., Medved, L. V., Henschen, A. H., and Weisel, J. W. (1994) *Biochemistry* **33**, 6986–6997
- Shainoff, J. R., and Dardik, B. N. (1979) *Science* **204**, 200–204
- Mosesson, M. W., DiOrto, J. P., Müller, M. F., Shainoff, J. R., Siebenlist, K. R., Amrani, D. L., Homandberg, G. A., Soria, J., Soria, C., and Samama, M. (1987) *Blood* **69**, 1073–1081